Polycyclic Aromatic Hydrocarbons Hot Paper

How to cite: Angew. Chem. Int. Ed. 2021, 60, 26346–26350
International Edition: doi.org/10.1002/anie.202110311
German Edition: doi.org/10.1002/ange.202110311

An on-surface Diels–Alder reaction

Jesús Castro-Esteban[+], Florian Albrecht[+], Shadi Fatayer, Dolores Pérez, Leo Gross, and Diego Peña**

Dedicated to Professor Tomás Torres on the occasion of his 70th birthday

Abstract: *The Diels–Alder reaction is one of the most popular reactions in organic chemistry. However, its use in the field of on-surface synthesis is hampered by the spatial restrictions of this cycloaddition reaction. Herein we selected a cyclic strained triyne to demonstrate an on-surface hexadehydro-Diels–Alder reaction in a single molecule. The reaction was studied in detail by means of atomic force microscopy (AFM) with CO-functionalized tips. Our results pave the way to use this iconic pericyclic reaction for on-surface synthesis, introducing the concept of atom economy in the field.*

The Diels–Alder (DA) reaction is one of the most important reactions in chemistry. In this [4+2] cycloaddition, the reaction between a diene (4π electrons) and a dienophile (2π electrons) generates a new six-membered ring by forming two new σ-bonds between the reaction partners (Figure 1 a). First reported in 1928 by Otto Diels and Kurt Alder while studying the products from the reaction of cyclopentadiene with quinone,[1] in few years the Diels–Alder reaction became one of the most popular reactions in organic synthesis.[2] According to Roald Hoffman, the distinguished pioneer in the study of organic reactivity, the relevant role of the DA reaction is due to "…the economy it brings to synthesis, and the frequency of the six-membered ring in organic chemistry".[3]

In the last years, impressive progress has been made in the field of on-surface synthesis, spurred by pioneering works of Grill, Hecht and co-workers,[4,5] and carbon nanoribbons discovered by Fasel, Müllen and co-workers.[6] In recent years, a plethora of reactions has been induced on different surfaces and visualized by scanning probe microscopy (SPM) with submolecular resolution, including Ullmann couplings, alkyne cyclizations, cyclodehydrogenations, Glaser couplings and Bergman cyclizations, among other interesting transformations.[7] However, despite the privileged role of the DA reaction in organic chemistry and the demonstration of other cycloaddition reactions on surface,[8–14] there are very few reports about on-surface transformations based on DA reactions.[15,16] As remarkable exceptions, Jelínek, Starý and co-workers proposed a Diels–Alder reaction to describe the planarization of a heptahelicene derivative on Ag(111),[16a] while Müllen, Fasel and co-workers suggested a dehydro-Diels–Alder cycloaddition as part of a reaction sequence to explain the thermal oligomerization of bis(phenylethynyl)-benzene derivatives on Au(111).[16b] In the latter, the on-surface cyclization proceeded between planar moieties on the surface, where diene and dienophile approach each other within the same plane. This is in contrast with the conventional DA reaction where the approach is along staggered parallel planes. The spatial restrictions due to the adsorption of the reactants on the surface, limit the possibilities to study and use the DA reaction for on-surface chemistry. Herein, we describe our efforts to induce and investigate an on-surface DA reaction in a single molecule, facilitated by the careful design of the precursor molecule.

Initially, we began searching for a suited molecular system to study the on-surface DA reaction, bearing in mind some important restrictions. First, as commented above, the conventional DA reaction requires that both diene and dien-

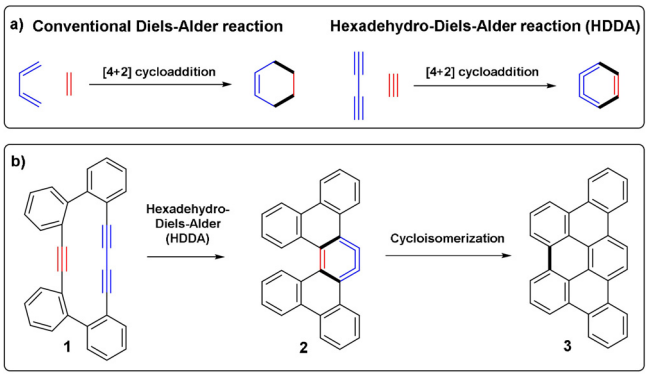

Figure 1. a) Representation of Diels–Alder (DA) and hexadehydro-Diels–Alder (HDDA) reactions. b) HDDA reaction studied on surface in this work.

[*] J. Castro-Esteban,[+] Prof. Dr. D. Pérez, Prof. Dr. D. Peña
Centro Singular de Investigación en Química Biolóxica e Materiais Moleculares (CiQUS) and Departamento de Química Orgánica, Universidade de Santiago de Compostela
15782-Santiago de Compostela (Spain)
E-mail: diego.pena@usc.es
Dr. F. Albrecht,[+] Dr. S. Fatayer, Dr. L. Gross
IBM Research—Zurich
8803 Rüschlikon (Switzerland)
E-mail: LGR@zurich.ibm.com
[+] These authors contributed equally to this work.
Supporting information and the ORCID identification number(s) for the author(s) of this article can be found under: https://doi.org/10.1002/anie.202110311.

ophile approach each other from different planes and in a concerted way, which complicates the possibility to perform this reaction on surface. Second, the reaction product is frequently a non-planar molecule, which renders it difficult to identify and study it by SPM. Third, the activation energy involved in the conventional DA reaction may be relatively high. Due to these restrictions, we focused our attention on the hexadehydro-Diels–Alder (HDDA) reaction,[17–20] a [4+2] cycloaddition between a diyne and an alkyne to form an aryne (Figure 1 a), that is, a highly reactive flat molecular species that is stable under UHV conditions and can be studied by SPM, as previously shown by some of us.[21] In particular, a properly designed triyne moiety combining both reaction partners, could provide enough ring strain to facilitate an intramolecular HDDA, affording a planar product that could be identified by SPM.

Inspired by the work of Tobe and co-workers,[22] we studied the intramolecular HDDA reaction of triyne **1** on surface (Figure 1 b). This compound is a twisted biphenylophane with a highly distorted diacetylene moiety that could facilitate the on-surface HDDA reaction, leading to the formation of aryne **2**. This particular transformation was previously reported in solution,[22] the aryne **2** being intercepted by reaction with furan. On-surface, we expect that aryne **2** could evolve by cycloisomerization to obtain tribenzo[*fg,ij,rst*]pentaphene (**3**), a flat aromatic hydrocarbon that might be unambiguously identified by AFM to demonstrate the on-surface HDDA reaction.

First, we prepared triyne **1** following the synthetic procedure previously reported (see supporting information (SI) for details, Figure S1 and S2).[22] We evaporated triyne **1** by flash heating from a silicon wafer piece onto a Cu(111) single crystal, partially covered by bilayer NaCl islands, at a sample temperature of $T \approx 10$ K. The AFM tip was functionalized by picking up an individual CO molecule from bilayer NaCl (see SI, Figure S3).[23] All measurements shown were obtained with a CO functionalized tip on molecules adsorbed on Cu(111) at $T = 5$ K. AFM and STM data of molecules observed after preparation at $T = 10$ K, without post annealing, are shown in Figure 2. We observed molecules with qualitatively different contrasts that we assigned to different adsorption conformations (and enantiomers) of **1** on Cu(111), with the aid of density functional theory (DFT) calculations and AFM simulations (see SI).[24] We found that **1** was adsorbed either with a diyne group (Figure 2 a) or a monoyne group (Figure 2 e, i), in contact with the Cu substrate. Then the opposing group (i.e., monoyne or diyne, respectively) was exposed towards the tip and showed a characteristic contrast in AFM measurements. The contrast of the exposed triple bonds is resolved as bright features in AFM acquired at a tip height that corresponds to the onset of atomic resolution (see Figure 2 c, g, k), explained by their high electron density.[25–27] Furthermore, we distinguish two different adsorption conformations of the monoyne group in contact to the Cu sample. Most clearly, they are distinguished with AFM at small tip heights, shown in Figure 2 h and l, and they show different adsorption heights (see SI, Figure S4–S7). We assigned the former to a physisorbed species (physisorbed monoyne) and the latter to a chemisorbed species (chemisorbed monoyne). For the molecules with diyne in contact to Cu, we find only one conformation that we assigned to molecules that are chemisorbed with a diyne group to the Cu(111) substrate (Figure 2 a). The most abundant species found was the latter, that is, chemisorbed diyne (see SI, Figure S5 for DFT calculations). Note that compound **1** is a helical twisted chiral hydrocarbon and we found both enantiomers *M* and *P* (with similar occurrences), in each of the three adsorption conformations, yielding in total six observed adsorption geometries (see SI, Figure S4). Also, the products discussed in the following, are chiral molecules,

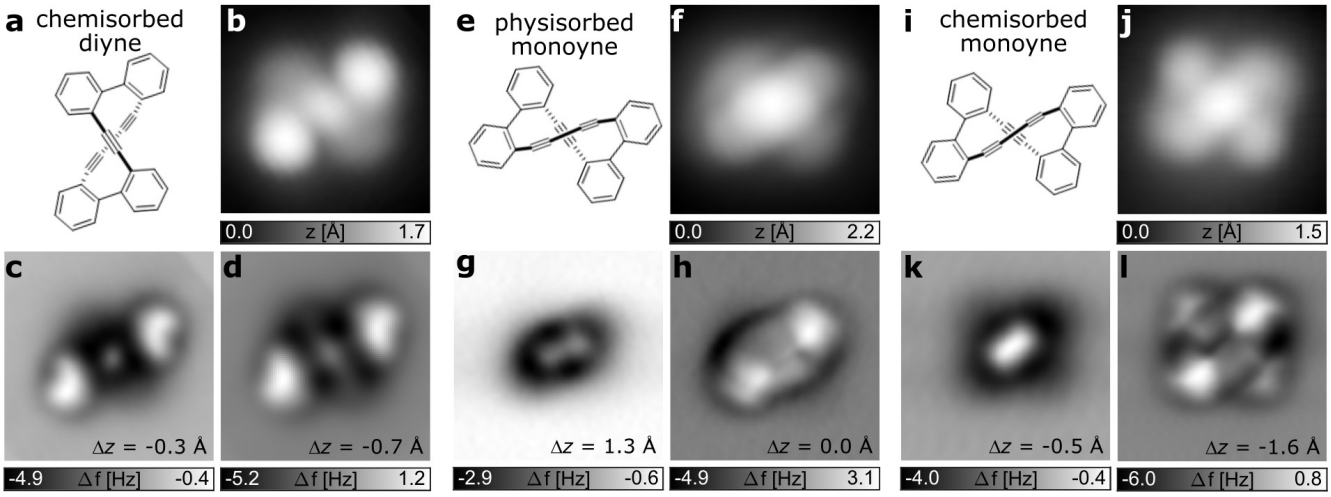

Figure 2. Molecular models and experimental data for triyne **1**, prepared on Cu(111) at $T = 10$ K without post annealing. We assigned the adsorption geometries as chemisorbed diyne (P)-**1** (a–d), physisorbed monoyne (M)-**1** (e–h) and chemisorbed monoyne (M)-**1** (i–l). Corresponding experimental constant-current STM images (b, f, j) at $I = 1$ pA and $V = 0.1$ V, and constant-height AFM images (c, d, g, h, k, l) at tip heights Δz with respect to the STM setpoint ($I = 1$ pA, $V = 0.1$ V) on bare copper indicated. All images are 20 Å by 20 Å. The three adsorption conformations are shown exemplarily for one enantiomer here. For both *M* and *P* enantiomers of **1** we observed all three adsorption conformations. The prevalently observed adsorption conformation was the chemisorbed diyne.

except for the final product **3**. We always found both enantiomers with similar occurrences indicating racemic mixtures and do not discuss enantiomers separately.

When we annealed the sample to 463 K, we observed structure **3′**, shown in Figure 3 a–c, as the prevalent molecule on the surface. After annealing to 558 K we observed structure **3**, shown in Figure 3 d–f as the only species. Note that compound **3′**, which we assigned to a π-radical, could also be transformed into **3** by atom manipulation, that is, by applying a voltage pulse above **3′** with a voltage of $V = 4.2$ V and $30\ \text{pA} < I < 250\ \text{pA}$, to dissociate the hydrogen atom bonded to the sp^3 hybridized carbon,[28,29] breaking the weakest bond of the molecule.

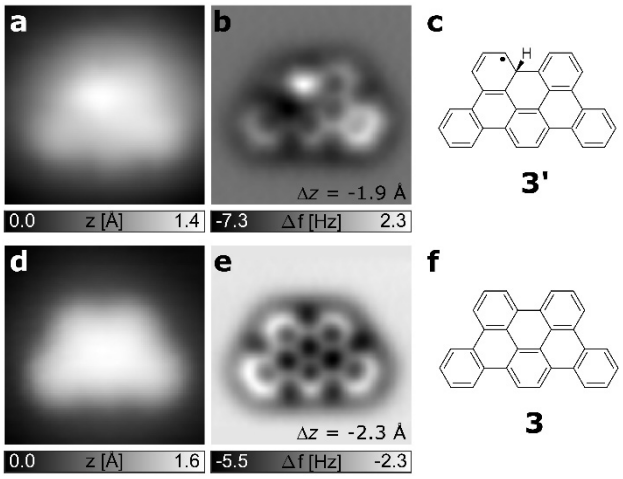

Figure 3. Planar products after annealing. (a–c) Prevalent adsorbate on the Cu(111) surface after annealing to 463 K. (d–f) Only adsorbate on the Cu(111) surface after annealing to 558 K. (a, d) Constant-current STM data, $V = 0.1$ V and $I = 1$ pA in (a), $I = 10$ pA in (b); (b, e) constant-height AFM data with Δz indicated; (c, f) molecular models. All images are 20 Å by 20 Å.

The final product **3** is a planar polycyclic aromatic hydrocarbon (PAH) rendering its assignment with AFM very certain. Note that also the hydrogenation of the carbons at the periphery can be inferred from the AFM data, as hydrogen atoms are observed as additional protrusions,[28] while reactive sites (σ-radicals with missing hydrogen) lead to bond formation to the Cu substrate and in turn to tilted adsorption geometries,[28,21] and in addition to subtle changes in bond order relations.[21] In turn, we assigned with high certainty the intermediate found after annealing to 463 K as **3′** (see SI, Figure S8 for AFM simulations), which is the final reaction product **3** with one additional hydrogen atom. The finding of these structures evidences the transformation of **1** into **3** and suggests that a Diels–Alder reaction was thermally induced on surface.

To increase our insight into the reaction pathway, we were looking for additional intermediates and conducted experiments in which the sample had been annealed to maximal temperatures of 413 K and 423 K. After such maximal annealing temperatures, we found several different non-planar species with significant occurrences on the surface, with the most abundant ones shown in Figure 4. Because of

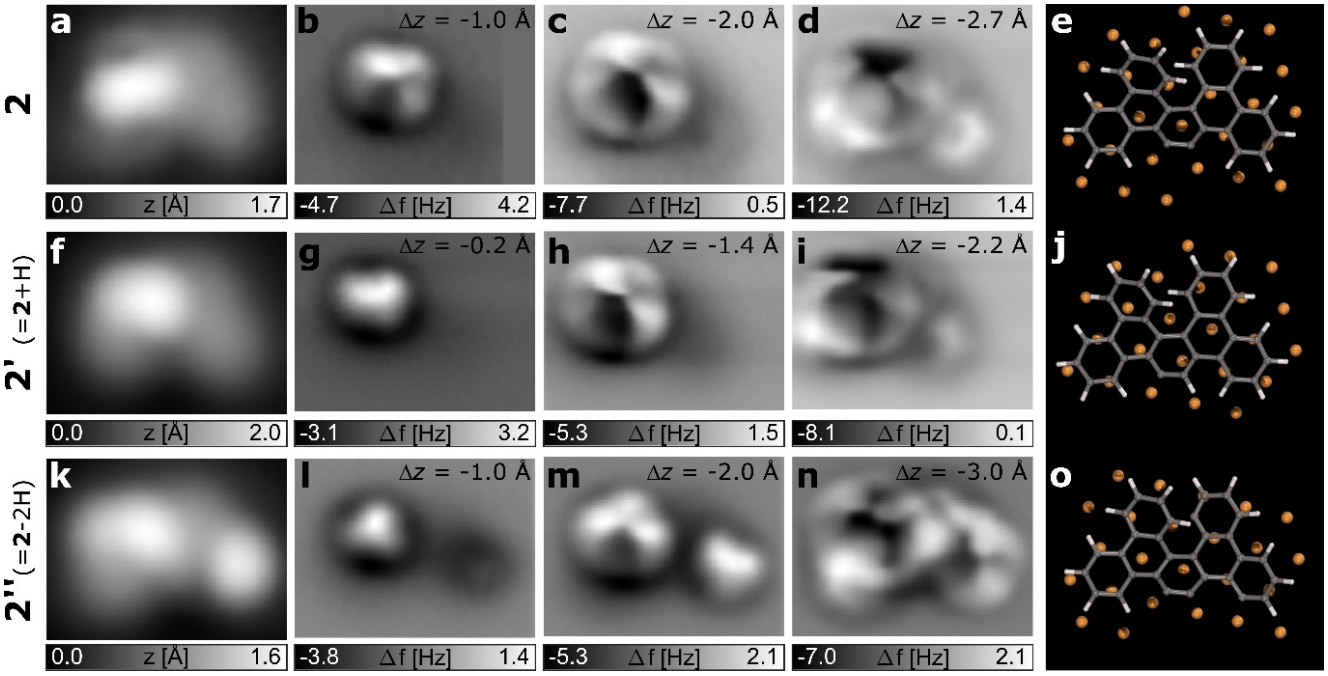

Figure 4. Intermediates observed on Cu(111) after annealing the sample to 413 K and 423 K. We observed species with three characteristically different contrasts shown in the three rows. STM images (a, f, k) at $I = 1$ pA, $V = 0.1$ V. (b–d, g–i, l–n) AFM images of the respective molecules, at different Δz. We tentatively assign the intermediates as shown in the models (e,j,o): Structure **2** (e) as the anticipated product after a HDDA reaction of **1**, with all hydrogen atoms still attached to the same carbons as in the precursor **1**; structure **2′** (j) as the HDDA product of **1** with an additional H atom at the aryne moiety; structure **2″** (o) as the HDDA product of **1** with two hydrogen atoms of one phenanthrene moiety dissociated. All images are 20 Å by 15 Å.

their non-planarity and their reduced symmetry, compared to **1** and **3**, the assignment of the structures is challenging. In addition to the STM and AFM images at different height we performed $\Delta f(z)$ spectroscopy (see SI, Figure S9) and we used DFT to calculate adsorption geometries of different structures and AFM simulations for those. We tentatively assign the structures as shown by the models in Figure 4.

The structure shown in the first row of Figure 4 we tentatively assigned to **2** (Figure 4e), i.e., the aryne that is the anticipated product after a Diels–Alder reaction, with all hydrogen atoms still attached to the same carbons as in the precursor **1**. In addition, we found molecules that exhibit a characteristically different contrast in both STM and AFM. Based on DFT calculations and AFM simulations, we tentatively assigned the structure imaged in the second row as compound **2′** (Figure 4j), which corresponds to **2** with an additional H atom attached to one of the carbon atoms of the aryne moiety and the structure in the third row of Figure 4 to compound **2″** (Figure 4o), which corresponds to aryne **2** but with two hydrogen atoms dissociated from one phenanthrene moiety (see SI, Figure S10 for AFM simulations of other possible intermediates).

Statistics of the counted species after the different maximal annealing temperatures are shown in Table 1. After annealing to 413 K, we found that **2** was the prevalent compound, whereas for 423 K, **2″** was the prevalent species. However, at annealing temperatures of both 413 K and 423 K all three structures **2**, **2′** and **2″** coexisted with significant occurrences.

In contrast to on-surface Ullmann or Glaser type coupling reactions the number of atoms in precursor **1** and product **3** is identical, which relates to the atom economy of the DA reaction.[3] However, the number of hydrogen atoms is not conserved in the complete reaction pathway. Structure **3′**, which is found with an abundance of 86 % after annealing to 463 K, contains one hydrogen atom more than both the precursor **1** and the final product **3**. The coexistence of the tentatively assigned intermediates **2**, **2′** and **2″** would indicate intermolecular hydrogen migration, which has been frequently described in on-surface chemistry,[30] and might be important in the reaction pathway.

The important finding of this work is the HDDA cyclization reaction of **1**. The structure of the anticipated product **2** could only be assigned tentatively and with some uncertainty, as also other similar products are possible and have also been tentatively assigned (**2′** and **2″**). However, the certain assignment of the reaction products **3′** and **3** formed at elevated temperatures, provides strong evidence for the on-surface HDDA cyclization of **1**.

In conclusion, we have demonstrated an intramolecular on-surface hexadehydro-Diels–Alder reaction, indicating that this important type of transformation is energetically favored and can be triggered with high yield by thermal activation on surface. More insights about the Diels–Alder reaction could be obtained by cleverly designed precursor molecules and AFM investigations after different annealing steps. On-surface intermolecular Diels–Alder reactions could lead to novel nanostructures and an improved atom economy in on-surface synthesis.

Table 1: Relative occurrences in % of observed structures as a function of maximal annealing temperature.[a]

Structure	Maximal annealing temperature				
	10 K	413 K	423 K	463 K	558 K
1	100	0	0	0	0
2	0	46	15	3	0
2′	0	31	26	0	0
2″	0	17	54	0	0
3′	0	0	0	86	0
3	0	0	0	3	100
unassigned	0	6	5	8	0

[a] The first column corresponds to the sample that was prepared at $T = 10$ K inside the microscope without post annealing. In the other columns, the sample had been annealed on the manipulator to the indicated maximum temperature. For **1** at $T = 10$ K, three different adsorption conformations can be distinguished (see Figure 2), i.e., chemisorbed diyne, physisorbed monoyne and chemisorbed monoyne, which were observed in the ratio 9:3:2, respectively. The total numbers of observed individual molecules were 56, 54, 100, 72 and 20 in the columns from 10 K to 558 K, respectively.

Acknowledgements

We thank Rolf Allenspach and Enrique Guitián for discussions. We thank the European Union (Project SPRING, contract no. 863098), the ERC grant AMSEL (682144), the Spanish Agencia Estatal de Investigación (PID2019-107338RB-C62, PID2019-110037GB-I00 and PCI2019-111933-2), Xunta de Galicia (Centro de Investigación de Galicia accreditation 2019–2022, ED431G 2019/03) and the European Regional Development Fund-ERDF for financial support.

Conflict of Interest

The authors declare no conflict of interest.

Keywords: bond-resolved AFM · cycloaddition · Diels–Alder reaction · on-surface synthesis · polycyclic aromatic hydrocarbons

[1] O. Diels, K. Alder, *Justus Liebigs Ann. Chem.* **1928**, *460*, 98–122.
[2] K. C. Nicolaou, S. A. Snyder, T. Montagnon, G. Vassilikogiannakis, *Angew. Chem. Int. Ed.* **2002**, *41*, 1668–1698; *Angew. Chem.* **2002**, *114*, 1742–1773.
[3] K. N. Houk, F. Liu, Z. Yang, J. I. Seeman, *Angew. Chem. Int. Ed.* **2021**, *60*, 12660–12681; *Angew. Chem.* **2021**, *133*, 12768–12790.
[4] L. Grill, M. Dyer, L. Lafferentz, M. Persson, M. V. Peters, S. Hecht, *Nat. Nanotechnol.* **2007**, *2*, 687–691.
[5] L. Lafferentz, F. Ample, H. Yu, S. Hecht, C. Joachim, L. Grill, *Science* **2009**, *323*, 1193–1197.
[6] J. Cai, P. Ruffieux, R. Jaafar, M. Bieri, T. Braun, S. Blankenburg, M. Muoth, A. P. Seitsonen, M. Saleh, X. Feng, K. Müllen, R. Fasel, *Nature* **2010**, *466*, 470–473.
[7] S. Clair, D. G. de Oteyza, *Chem. Rev.* **2019**, *119*, 4717–4776.

[8] F. Bebensee, C. Bombis, S.-R. Vadapoo, J. R. Cramer, F. Besenbacher, K. V. Gothelf, T. R. Linderoth, *J. Am. Chem. Soc.* **2013**, *135*, 2136 – 2139.
[9] O. Díaz Arado, H. Mönig, H. Wagner, J.-H. Franke, G. Langewisch, P. A. Held, A. Studer, H. Fuchs, *ACS Nano* **2013**, *7*, 8509 – 8515.
[10] C. Sánchez-Sánchez, A. Nicolai, F. Rossel, J. Cai, J. Liu, X. Feng, K. Müllen, P. Ruffieux, R. Fasel, V. Meunier, *J. Am. Chem. Soc.* **2017**, *139*, 17617 – 17623.
[11] B. V. Tran, T. A. Pham, M. Grunst, M. Kivala, M. Stöhr, *Nanoscale* **2017**, *9*, 18305 – 18310.
[12] Q. Li, J. Gao, Y. Li, M. Fuentes-Cabrera, M. Liu, X. Qiu, H. Lin, L. Chi, M. Pan, *Nat. Commun.* **2018**, *9*, 3113.
[13] M. Koch, M. Gille, S. Hecht, L. Grill, *Surf. Sci.* **2018**, *678*, 194 – 200.
[14] R. Zuzak, O. Stoica, R. Blieck, A. M. Echavarren, S. Godlewski, *ACS Nano* **2021**, *15*, 1548 – 1554.
[15] a) For a DA reaction studied by a scanning tunnelling microscopy break-junction approach, see: A. C. Aragonès, N. L. Haworth, N. Darwish, S. Ciampi, N. J. Bloomfield, G. G. Wallace, I. Diez-Perez, M. L. Coote, *Nature* **2016**, *531*, 88 – 91; b) For a DA reaction between a polyarene and a semiconductor surface, see: S. Godlewski, M. Engelund, D. Peña, R. Zuzak, H. Kawai, M. Kolmer, J. Caeiro, E. Guitián, K. P. C. Vollhardt, D. Sánchez-Portal, M. Szymonski, D. Pérez, *Phys. Chem. Chem. Phys.* **2018**, *20*, 11037 – 11046.
[16] a) O. Stetsovych, M. Švec, J. Vacek, J. V. Chocholoušová, A. Jančařík, J. Rybáček, K. Kosmider, I. G. Stará, P. Jelínek, I. Starý, *Nat. Chem.* **2017**, *9*, 213 – 218; b) M. Di Giovannantonio, A. Keerthi, J. I. Urgel, M. Baumgarten, X. Feng, P. Ruffieux, A. Narita, R. Fasel, K. Müllen, *J. Am. Chem. Soc.* **2020**, *142*, 1721 – 1725.
[17] A. Z. Bradley, R. P. Johnson, *J. Am. Chem. Soc.* **1997**, *119*, 9917 – 9918.
[18] K. Miyawaki, R. Suzuki, T. Kawano, I. Ueda, *Tetrahedron Lett.* **1997**, *38*, 3943 – 3946.
[19] T. R. Hoye, B. Baire, D. Niu, P. H. Willoughby, B. P. Woods, *Nature* **2012**, *490*, 208 – 212.
[20] X. Ma, J. Maier, M. Wenzel, A. Friedrich, A. Steffen, T. B. Marder, R. Mitric, T. Brixner, *Chem. Sci.* **2020**, *11*, 9198 – 9208.
[21] N. Pavliček, B. Schuler, S. Collazos, N. Moll, D. Pérez, E. Guitián, G. Meyer, D. Peña, L. Gross, *Nat. Chem.* **2015**, *7*, 623 – 628.
[22] S. Nobusue, H. Yamane, H. Miyoshi, Y. Tobe, *Org. Lett.* **2014**, *16*, 1940 – 1943.
[23] L. Gross, F. Mohn, N. Moll, P. Liljeroth, G. Meyer, *Science* **2009**, *325*, 1110 – 1114.
[24] P. Hapala, G. Kichin, C. Wagner, F. S. Tautz, R. Temirov, P. Jelínek, *Phys. Rev. B* **2014**, *90*, 085421.
[25] L. Gross, F. Mohn, N. Moll, B. Schuler, A. Criado, E. Guitián, D. Peña, A. Gourdon, G. Meyer, *Science* **2012**, *337*, 1326 – 1329.
[26] N. Pavliček, P. Gawel, D. R. Kohn, Z. Majzik, Y. Xiong, G. Meyer, H. L. Anderson, L. Gross, *Nat. Chem.* **2018**, *10*, 853 – 858.
[27] K. Kaiser, L. M. Scriven, F. Schulz, P. Gawel, L. Gross, H. L. Anderson, *Science* **2019**, *365*, 1299 – 1301.
[28] B. Schuler, W. Liu, A. Tkatchenko, N. Moll, G. Meyer, A. Mistry, D. Fox, L. Gross, *Phys. Rev. Lett.* **2013**, *111*, 106103.
[29] H. Hayashi, J. Yamaguchi, H. Jippo, R. Hayashi, N. Aratani, M. Ohfuchi, S. Sato, H. Yamada, *ACS Nano* **2017**, *11*, 6204 – 6210.
[30] a) C. Wäckerlin, A. Gallardo, A. Mairena, M. Baljozović, A. Cahlík, A. Antalík, J. Brabec, L. Veis, D. Nachtigallová, P. Jelínek, K.-H. Ernst, *ACS Nano* **2020**, *14*, 16735 – 16742; b) C. Wäckerlin, *Angew. Chem. Int. Ed.* **2021**, *60*, 8446 – 8449; *Angew. Chem.* **2021**, *133*, 8527 – 8530.

Manuscript received: August 2, 2021
Revised manuscript received: October 10, 2021
Accepted manuscript online: October 19, 2021
Version of record online: November 10, 2021

